

# **Refining Surface Net Radiation Estimates in Arid and Semi-Arid Climates of Iran**

Foroogh Golkar<sup>a</sup>, William B. Rossow<sup>b</sup> and Ali Akbar Sabziparvar<sup>c\*</sup>

*<sup>a</sup>Ph.D Candidate of Agricultural Meteorology, Bu-Ali Sina University, Hamedan 65178, Iran,  
and Research Scholar at NOAA-CREST Institute at City College of New York, NY, USA  
foroogh.golkar@gmail.com*

*<sup>b</sup> CREST Institute at City College of New York, NY, USA ; wbrossow@ccny.cuny.edu*

*<sup>c</sup> Professor in Meteorology, Bu-Ali Sina University, Faculty of Agriculture, Hamedan, 65178,  
Iran.*

*\*Correspondence: e-mail:swsabzi@basu.ac.ir; Tel. +98 81 38273001*

# **Refining Surface Net Radiation Estimates in Arid and Semi-Arid Climates of Iran**

## **Abstract**

Although the downwelling fluxes exhibit space-time scales of dependency on characteristic of atmospheric variations, especially clouds, the upward fluxes and, hence the net radiation, depends on the variation of surface properties, particularly surface skin temperature and albedo. Evapotranspiration at the land surface depends on the properties of that surface and is determined primarily by the net surface radiation, mostly absorbed solar radiation. Thus, relatively high spatial resolution net radiation data are needed for evapotranspiration studies. Moreover, in more arid environments, the diurnal variations of surface (air and skin) temperature can be large so relatively high (sub-daily) time resolution net radiation is also needed. There are a variety of radiation and surface property products available but they differ in accuracy, space-time resolution and information content. This situation motivated the current study to evaluate multiple sources of information to obtain the best net radiation estimate with the highest space-time resolution from ISCCP FD dataset. This study investigates the accuracy of the ISCCP FD and AIRS surface air and skin temperatures, as well as the ISCCP FD and MODIS surface albedos and aerosol optical depths as the leading source of uncertainty in ISCCP FD dataset. The surface air temperatures, 10-cm soil temperatures and surface solar insolation from a number of surface sites are used to judge the best combinations of data products., especially on clear days. The corresponding surface skin temperatures in ISCCP FD, although they are known to be biased somewhat high, disagreed more with AIRS measurements because of the mismatch of spatial resolutions. The effect of spatial resolution on the comparisons was confirmed using the even higher resolution MODIS surface skin temperature values. The agreement of ISCCP FD surface solar insolation with surface measurements is good (within 2.4 - 9.1%), but the use of MODIS aerosol optical depths as an alternative was checked and found to not improve the agreement. The MODIS surface albedos differed from the ISCCP FD values by no more than

0.02 - 0.07, but because these differences are mostly at longer wavelengths, they did not change the net solar radiation very much. Therefore to obtain the best estimate of surface net radiation with the best combination of spatial and temporal resolution, we developed a method to adjust the ISCCP FD surface longwave fluxes using the AIRS surface air and skin temperatures to obtain the higher spatial resolution of the latter (45 km), while retaining the 3-hr time intervals of the former. Overall, the refinements reduced the ISCCP FD longwave flux magnitudes by about 25.5- 42.1 W/m<sup>2</sup>RMS (maximum difference - 27.5 W/m<sup>2</sup> for incoming longwave radiation and -59 W/m<sup>2</sup> for outgoing longwave radiation) with the largest differences occurring at 9:00 and 12:00 UTC near local noon. Combining the ISCCP FD net shortwave radiation data and the AIRS-modified net longwave radiation data changed the total net radiation for summertime by 4.64 to 61.5 W/m<sup>2</sup> and for wintertime by 1.06 to 41.88 W/m<sup>2</sup> (about 11.1 to 39.2 % of the daily mean).

Keywords: Net Radiation Flux; ISCCP FD Dataset; AIRS; MODIS

## **1. Introduction**

Land surface evapotranspiration (ET) models routinely use solar radiation directly or, in combination with longwave radiation, the net radiation (R<sub>n</sub>) to provide a measure of the net energy available to evaporate water (Boegh et al., 2002; Monteith, 1965; Nishida et al., 2003; Priestley and Taylor, 1972; Shuttleworth and Wallace, 1985; Su, 2002). Many of these ET models prefer knowledge of the diurnal cycle of net radiation at high spatial resolution.

Variation of the downwelling components of net radiation (R<sub>n</sub>) is dominated by atmospheric variations, primarily clouds and temperature, but the upwelling components depend on the variation of surface properties. The advent of satellite measurements of atmosphere and surface properties has led to estimates of surface radiative fluxes that can cover this large range of space-time scales. However, the usefulness of these flux products is dependent on three issues: (1) the uncertainty of the calculated radiative fluxes as judged by comparison with more direct measurements, (2) the space-time scales

available in these products, and (3) how much and by what means the flux products can be improved. (Zhang et al., 2004, 1995) estimated their overall surface flux uncertainty at about 10–15 W/m<sup>2</sup> for surface fluxes. More importantly, they conducted comprehensive sensitivity studies by varying the input data sets (and the radiative transfer model parameters) to quantify the uncertainties associated with each input quantity. The main conclusion was that the advent of extensive cloud data sets has reduced role of clouds as the main source of uncertainty in downwelling surface fluxes, making other uncertainty sources relatively more important. For surface radiative flux estimates, the accuracy of the near-surface atmospheric radiative properties (temperature, humidity and aerosol optical depth) are key for downwelling fluxes and the surface radiative properties (surface skin temperature and solar albedo) are key for upwelling fluxes (Zhang et al., 2007, 2006, 2004).

Our study area is the Fars Province in southern Iran (surface area of 122,608 km<sup>2</sup>, one of the largest Iranian provinces), which is known for its semi-arid climate and flourishing agriculture. To study the effects of surface property variations and/or changes on the water budget in a semi-arid environment, evapotranspiration models, such as the Priestley-Taylor equation, can be used for this purpose if relatively high space-time resolution surface net radiation data can be obtained, but lack of sufficient ground-based data almost always is known as the main limitation. The radiation data from ISCCP FD dataset (Zhang et al., 2004) has the desired time resolution (3-hour intervals) but the spatial resolution is coarse (280 km), providing only five values for the whole province. In order to improve the spatial resolution of surface radiative fluxes from ISCCP FD dataset, the pressing problem is evidently to improve the input data resolution as well as its accuracy. Our investigation of the accuracy of the ISCCP FD fluxes by comparisons with other satellite data products, as well as surface station measurements, shows that the fluxes are accurate enough that, rather than starting from the beginning to calculate new fluxes with better inputs, we can adjust the ISCCP FD fluxes directly based on alternate inputs. The additional benefit is to increase the spatial sampling interval to provide more detail, while no sufficient ground-based measurements are available for net flux in the study area. Thus, that is the main point of the current study to

improve a method in refining spatial resolution as well as accuracy of the ISCCP FD fluxes, using satellite products, where in principle, provide the needed data for our study.

## **2. Data sets and methods**

### ***2.1. Study area and data***

In the Fars Province 16 automatic weather stations (AWS) in 2009 are selected for this study because they have the most complete information and most nearly complete time records (Figure 1). These stations record near-surface air temperature ( $T_a$  at 2 m height), soil temperature ( $T_{10}$  at 10 cm depth) and incoming shortwave radiation (SW) every 10 minutes. The selection of this kind of station is aimed at evaluating the data at the time of satellite overpass with maximum 5 minutes from the surface measurements.

The global radiation pyranometer with spectral range of 300- 3000 nm is used in all AWS. We use these data to evaluate  $T_a$  and, indirectly, surface skin temperature ( $T_s$ ) data from ISCCP FD, AIRS and  $T_s$  from MODIS - the main factors determining surface LW fluxes - and to evaluate the effects of surface albedo ( $A_s$ ) and aerosol optical depth (AOD) on the SW fluxes from ISCCP FD. Note that the lack of direct surface measurements of  $T_s$  means that we can only check the qualitative consistency of the satellite values by comparison with the station soil temperature at 10 cm depth: the expectation is that during daytime, especially in summer, the value of  $T_s$  will generally be larger than both  $T_a$  and  $T_{10}$  and during nighttime, especially in winter, the value of  $T_s$  will generally be smaller than  $T_a$  and  $T_{10}$  (Arya, 2001). All data are from 2009 in this study.

The International Satellite Cloud Climatology Project (ISCCP) cloud data products (Rossow and Schiffer, 1991) describe the variations of the key physical attributes of the clouds, atmosphere and surface that affect the radiation balance. These observations are input to a radiative transfer model from the GISS GCM (revised) to calculate upwelling and downwelling, total shortwave (SW = 0.2 - 5  $\mu\text{m}$  wavelength)

and total longwave (LW = 5 - 200  $\mu\text{m}$  wavelength) radiative fluxes at five levels: surface, 680 mb, 440 mb, 100 mb and top-of-atmosphere (<http://isccp.giss.nasa.gov>), every three hours over the whole globe on a 280 km equal-area global grid for July 1983 – December 2009 (Zhang et al., 2004). The ISCCP FD dataset also includes the values of  $T_a$ ,  $T_s$ ,  $A_s$ , and monthly AOD used to calculate the fluxes. There are five ISCCP FD grids located in the Fars province, each of which contains at least one weather station (Figure 1).

AIRS (Atmospheric Infrared Sounder) sensor products, which is one of six instruments flying on board NASA's Aqua satellite, launched on May 2002, also reports values of  $T_a$  and  $T_s$  at 45 km intervals twice daily under clear to mostly clear conditions. Aqua passes over the Fars province at about 8:55-10:35 UTC (12:25-14:05 LST) and 21:30-23:20 UTC (01:00-02:50 LST) (<http://disc.sci.gsfc.nasa.gov/AIRS/data-holdings>). The local sidereal time is 3:30 ahead of UTC.

MODIS (Moderate Resolution Imaging Spectroradiometer) products from Terra and Aqua satellites include values of  $T_s$  (MOD11 and MYD11) under clear conditions,  $A_s$  (MCD43) and AOD (MOD04 and MYD04). AOD is reported at a spatial interval of 10 km and both  $T_s$  and  $A_s$  are reported at 1 km (<https://ladsweb.nascom.nasa.gov/>). Terra passes over the Fars province at about 6:25-8:10 UTC (09:55-11:40 LST) and 17:45-19:25 UTC (21:15-22:55 LST).

## ***2.2. Evaluating ISCCP FD quantities***

### ***2.2.1. Evaluating longwave radiation input data***

$T_s$  and  $T_a$  are the two dominant factors determining the upwelling and downwelling LW fluxes, respectively (Zhang et al., 1995). Only 2–4 K differences in temperatures can cause 15–30  $\text{W/m}^2$  differences in calculated surface LW fluxes (Zhang et al., 2007).

During daytime, as shown in Table 1, the ISCCP FD values of  $T_a$  compared to surface station measurements of  $T_a$  exhibits average differences between 3.5- 4.4 K and RMS differences between 5.4- 7.4 K (except in grid 5 which contains a substantial fraction of ocean). At nighttime, the average and rms

differences are 3.0-5.5 K and 5.0-7.0 K, respectively. Seasonal and monthly comparisons show slightly larger difference in wintertime and cold months especially January and February (see sec 3.1).Zhang et al., 2007 also reported the same result particularly in high latitudes (the worst disagreements reported over wintertime Antarctica).

Comparison of the surface skin temperatures from ISCCP FD with other measurements of related quantities suggests uncertainties of about 4 K over land; however, some differences are systematic with location and season can be somewhat larger in particular locations (Rossow and Garder, 1993).The surface measurement of soil temperature at 10 cm depth ( $T_{10}$ ) is the only available information for evaluating satellite values of  $T_s$ , qualitatively at least. The diurnal variation of solar heating of the surface skin and the lag time for the heat to penetrate into the surface should cause  $T_s$  to exceed both  $T_a$  and  $T_{10}$  during daytime, especially in summer, and to be about the same or less than  $T_a$  and  $T_{10}$  during nighttime especially in winter (Arya, 2001). The differences of ISCCP FD  $T_s$  and  $T_{10}$  are summarized in Table 2. In grids 1-4 the daytime average difference is between 11.0-14.0 K; in grid 5 (with ocean) the average difference is 1.0 K. At night the average difference is between (-2.7)-(-4.7) K; in grid 5 the average difference is 1.6 K. Thus, the ISCCP FD values of  $T_s$  meet expectations. In addition, the average of difference seems to be larger in summer daytime, while Zhang et al., 2007 reported both too cold  $T_s$  in winter and too warm during summertime. However, other investigations (Jimenez et al., 2012) shows that the ISCCP FD values of  $T_s$  tend to be biased slightly high, especially at the larger values in arid regions.

AIRS  $T_a$  and  $T_s$  data with 45 km resolution is compared to the surface station measurements (Table 1) and to ISCCP FD values. In daytime AIRS  $T_a$  shows an average of difference with surface measurements of -3.1 K and an RMS difference of 5.3 K. At night the average and RMS differences are -2.4 K and 4.6 K, respectively. AIRS  $T_s$  data compared with  $T_{10}$  (Table 2) shows an average daytime (nighttime) difference of 10.0 (-1.9) K and RMS differences of 9.1 (4.3) K. Thus, the AIRS  $T_s$  values are qualitatively consistent with measured  $T_a$  and  $T_{10}$ . AIRS  $T_a$  and  $T_s$  data comparison with ISCCP FD also confirms the tendency for ISCCP FD temperatures to be larger than AIRS temperatures.

MODIS  $T_s$  values with 1 km resolution (Table 2) show an average (RMS) of difference of 11.5(5.4)-12.6(12.9) K in daytime and -10.8(11.9) to -11.1(10.8) K at night for both Terra and Aqua datasets. The MODIS  $T_s$  values, although qualitatively consistent with surface-measured  $T_a$  and  $T_{10}$ , seem to be more extreme than the AIRS results: that the spatial match-up with the surface sites is better for MODIS than AIRS does not seem to improve the comparison. However, Jimenez et al., 2012 compared the LST from AIRS, MODIS and ISCCP FD in monthly time scale. They indicated AIRS and MODIS LSTs are closer to each other than they are to ISCCP LSTs, but some relatively large inconsistency can be seen in particular regions (e.g. over arid climate with high land surface temperatures).

For this reason and the fact that the MODIS product does not also have an associated (physically consistent) value of  $T_a$ , we focus our attention on AIRS, which seems to agree with the surface measurements slightly better than ISCCP FD.

For investigating the effect of topography on air and skin temperature differences, the correlation of the  $T_a$  and  $T_s$  average and RMS of differences with stations' elevation in monthly intervals was checked as well. The results show no systematic relationship between  $T_a$  differences (from ISCCP FD and AIRS) and  $T_s$  differences (from ISCCP FD, AIRS and MODIS) with elevation. The  $R^2$  value for  $T_a$  show the range of 0.0025-0.08 and it is 0.0063-0.042 for  $T_s$ .

We also investigated whether the slightly worse comparison of ISCCP FD temperatures with the surface measurements as compared to AIRS is affected by the lower spatial resolution of ISCCP FD. To this end we averaged the AIRS (and MODIS) values to the same resolution as ISCCP FD (280 km) and repeated the comparison to the surface measurements.

The resized-AIRS values of  $T_a$  are generally larger than the matched single field-of-view AIRS values for both daytime and nighttime and compare less well with the surface measurements (Table 1). The resized- AIRS  $T_s$  values in daytime (nighttime) are larger (smaller) than  $T_{10}$  values (Table 2), which is qualitatively correct; these differences are similar to those for the ISCCP FD values. We conclude that the resized-AIRS is less "accurate" than the 45 km resolution AIRS, but still a little more accurate than the ISCCP FD values (except in Grid 5). This means that some of the apparent disagreement between



ISCCP FD and the surface measurements is caused by the mis-matched spatial resolution. We also compared MODIS averaged to 45 km to AIRS and found that the disagreement did not change significantly. These results show that exploiting the higher spatial resolution of the AIRS products will improve the determination of surface fluxes, especially in grid 5 where the higher resolution reduces the mixing of ocean and land surfaces.

Since it is the difference of  $T_s$  and  $T_a$  that determines the net LW flux (Zhang et al., 2004), as well as the sensible heat flux, we also compared the values of  $\Delta T = (T_s - T_a)$  from ISCCP FD and AIRS. Since solar radiation in daytime tends to produce positive  $\Delta T$  and radiative cooling at night tends to produce nearly zero or negative  $\Delta T$ , we compare these two datasets for daytime and nighttime separately in yearly as well as seasonal and monthly time scale.

For the ISCCP FD dataset, daytime  $\Delta T$  values for each of the five grids are positive more than 75% of the time; nighttime  $\Delta T$  values for grids 1-4 are negative more than 53.8 % of the time (grid 5 has more positive values). Zhang et al., 2004 study in April 1992 (they chose the month with more scatter in both the polar regions), almost showed the same results with  $\Delta T$  values of mostly 2-3 K, while the reanalysis datasets showed slightly high biases (according to sensible heat transfer from surface to air).

The AIRS  $\Delta T$  values are almost completely negative at night and positive in daytime. Separating the cloudy and clear days and nights and focusing on clear conditions, the AIRS  $\Delta T$  values seem to be slightly more accurate than the ISCCP FD  $\Delta T$  values, especially during winter nighttime. This conclusion may be indicative of the fact that the AIRS  $\Delta T$  values are retrieved consistently from the same measurements, whereas the ISCCP FD values of  $T_a$  come from a different source than the values of  $T_s$ . AIRS histograms of  $\Delta T$  values during daytime and nighttime for winter and summer are presented in Figure 2.

### *2.2.2. Evaluating shortwave radiation input data*

The ISCCP FD downwelling SW fluxes at 3:00, 6:00, 9:00 and 12:00 UTC (local noon in the Fars Province is at 08:30 UTC) are compared with 3-hr averaged surface measurements since the ISCCP FD values represent 3-hr averages not samples (Zhang et al., 2004). The average differences in grids 1-4 vary from 2.37 to 9.1% (Table 3). The differences in grid 5 are larger (about 9.5- 16.5%) which may be associated with the large fraction of ocean in this grid. The maximum difference values occur at 3:00 UTC and the minimum at 9:00 UTC. Some bias in surface station data at 3:00 and even 15:00 UTC causes larger difference values at these times of day. Overall the downwelling SW flux differences are small but we investigate whether they can be improved by using a different AOD dataset as this was identified a leading source of uncertainty in the ISCCP FD values (Zhang et al., 2010). After that we check whether the surface net SW can be improved with a different (higher spatial resolution) surface albedo dataset.

The “Deep Blue” aerosol optical depth (AOD) retrieval algorithm was introduced in the MODIS Collection 5 product set, complementing the existing “Dark Target” land and ocean algorithms, by retrieving AOD over bright arid land surfaces, such as deserts. The new version of deep blue AOD (C6) extended coverage to vegetated surfaces, as well as bright land and is thought to be more accurate (Sayer et al., 2013). The AOD from the ISCCP FD dataset is available at monthly intervals and is based on a climatological compilation used in the NASA GISS climate model. MODIS daily AOD product comparison with mean monthly AOD from ISCCP FD ( $AOD_{ISCCP\ FD-monthly} - AOD_{MODIS-daily}$ ) showed the average differences of 0.129, 0.221, 0.290, 0.082, and 0.194 for grid 1 to 5 respectively. Also the monthly mean MODIS AOD, calculated from daily data and averaged over the ISCCP FD grids, is compared with the ISCCP FD AOD (using temporal average is a more appropriate comparison between ISCCP FD grid with satellite AOD data, called area-point comparison, so that the errors caused by the poor spatial match are somewhat reduced (Zhang et al., 2004)). The average differences vary from 0.035 to 0.189-with not very different from daily comparison. Overall the ISCCP FD AOD is greater than the MODIS AOD, except in some winter

months. The correlation between the difference of AOD from the two datasets with the difference between the ISCCP FD and the surface-measured downwelling SW fluxes in grid 1 (Figure 3) shows no systematic relationship. Similar results were found for the other grids. We conclude that there is not enough evidence to choose between these two AOD datasets; using the MODIS AOD would not improve the agreement with surface measurements of downwelling SW fluxes.

MODIS is the first imaging instrument with channels covering most of the solar spectral range so it can provide broadband and spectrally-resolved albedo values. The MODIS products provide both the white-sky values (bi-hemispherical reflectance, absence of a direct component) and the black-sky values (directional hemispherical reflectance, absence of a diffuse component) at local solar noon in MODIS bands 1-7 as well as for three broader bands (0.3-0.7 $\mu\text{m}$ , 0.7-5.0 $\mu\text{m}$ , and 0.3-5.0 $\mu\text{m}$ ). The ISCCP FD values are produced by combining the surface visible reflectances (wavelength about 0.65  $\mu\text{m}$ ) from the ISCCP cloud products (Rossow and Garder, 1993) and the NASA GISS GCM ratios of the NIR to visible albedo (Zhang et al., 1995). The ISCCP FD albedo values are compared with the MODIS MCD43B3 black-sky albedos, spatially-averaged to match the 280 km ISCCP FD grid. The results for grids 1, 2, 3 and 4 show that the average (RMS) differences (MODIS minus FD) vary from 0.02-0.07 (0.02-0.05). The difference in grid 5 is 0.15 when excluding the ocean from the MODIS value but much smaller when the ocean is included. Zhang et al. (Zhang et al., 2007) also compared the MODIS albedos with the ISCCP FD values and indicated that the differences appeared mostly in the NIR part of the spectrum. Since the atmosphere absorbs most of the SW radiation at these longer wavelengths, the effect of the albedo differences on the upwelling SW fluxes was small, average (RMS) differences over all land areas only  $-2.5$  (11)  $\text{W}/\text{m}^2$ . The results of the surface measurement comparisons and investigation of the AOD and surface albedo differences do not justify refining the ISCCP SW fluxes.

### **3. Results and discussion**

These comparisons of ISCCP FD and AIRS values of  $T_a$  and  $T_s$  (as well as MODIS  $T_s$ ) with surface measurements of  $T_a$  and  $T_{10}$  indicate that AIRS data shows better agreement, in part because of its higher spatial resolution (generally for all months and seasons during daytime and nighttime). However, the relatively small differences of the AIRS and ISCCP FD temperature values suggests that, rather than recalculating LW fluxes starting with AIRS data, we can adjust the ISCCP FD LW fluxes to account for the differences in  $T_s$  and  $T_a$  values. This approach is also necessitated by the fact that the AIRS temperature data has poorer time sampling (12-hr intervals) than the 3-hr sampling of the ISCCP FD data. This motivates our approach to merge the AIRS and ISCCP FD temperature information to obtain both 45-km and 3-hr values of  $T_a$  and  $T_s$  and to apply a small correction to the ISCCP FD LW fluxes based on the temperature differences.

### ***3.1. Merged ISCCP FD and AIRS analysis***

To improve both the spatial resolution as well as the accuracy of ISCCP FD LW fluxes while retaining its 3-hr time resolution, we use the differences between AIRS and ISCCP FD temperature values in each grid at each time to develop an adjustment for the ISCCP FD LW fluxes. The following equation is used to refine the ISCCP FD temperatures ( $T_a$  and  $T_s$ ):

$$T(t) = A + RB \tag{1}$$

where  $T(t)$  is either of the revised ISCCP FD temperatures at time of the day,  $t$ ,  $A$  is the daily average of the twice-daily AIRS values,  $R$  is daily ratio of difference of the two AIRS values to difference of the two ISCCP FD values at the same times of day, and  $B$  is the difference of ISCCP FD values at each time of day from the daily average. This correction is applied to each day of ISCCP FD temperature data. The LW adjustment to FD, applied to all time, both cloudy and clear sky by assuming the average change of the diurnal amplitude. Figure 4 illustrates the correction by showing the ISCCP FD temperatures on July 13, 2009 and the refined temperatures using AIRS data.

Table 4 shows the annual mean of  $T_a$  and  $T_s$  for ISCCP FD dataset and refined ISCCP FD dataset in each 3-hour interval for grids 1 and 5. The refined temperatures (both air and skin) are slightly smaller

compared to the original ISCCP FD dataset, except at 0:00, 3:00 and 21:00 UTC in grid 5. Overall, the differences between the refined and original temperatures vary from  $-5.3$  to  $0.9$  K for air temperature and from  $-9.5$  to  $-1.4$  K for surface skin temperature.

Figure 5 shows the relation between  $T_a$  and the downwelling LW flux and between  $T_s$  and the upwelling LW flux at 9:00 UTC for grid 1 (similar results found for the other grids). The larger scatter in the former relationship is caused by the additional dependence of the downwelling LW flux on water vapor and cloud variations. Since the temperature adjustments being made to the ISCCP FD temperatures are much smaller than the range of temperatures shown in Figure 5, a linear approximation can be used to adjust the ISCCP FD LW fluxes as functions of the change in temperatures. The yearly-average of the differences between the original and refined ISCCP FD downwelling LW fluxes vary from  $-27.5$  to  $2.5$   $W/m^2$  and the differences of upwelling LW fluxes vary from  $-9.7$  to  $-59$   $W/m^2$  in all 5 grids.

The above comparison was done for each month and season. Generally, both the refined  $T_a$ ,  $T_s$  and corresponding LW fluxes are smaller than the original values (except in grid 5), but there are some inconsistencies in wintertime for  $T_a$  and, thus, downwelling longwave radiation values in grids 3 and 4 at 0:00, 12:00, 15:00 and 21:00 UTC and in all 3-hour intervals in grid 5. The average of positive values of the difference between the refined and original ISCCP FD downwelling LW fluxes is  $4.8$   $W/m^2$  in grids 3 and 4. To investigate why these regions saw increased rather than decreased  $T_a$  values in winter, radiosonde data (at 0:00 UTC) was gathered from the only available station in the Fars Province at the Shiraz station located in grid 3. These temperature profiles show that throughout the winter there are frequent surface temperature inversions (only six days did not show this). These inversions extend from the surface to maximum heights of 225, 270 and 203 m in January, February and March, respectively. The temperature inversion magnitudes were about 1.5-13.0, 0.38-13.1 and 0.36-10.7 K/m, respectively. Zhang et al. (Zhang et al., 2006) also noted discrepancies in temperature profiles over winter land areas at high latitudes.

### ***3.2. Recalculating net radiation***

Net radiation is the sum of net shortwave radiation (NSW) and net longwave radiation (NLW). The refined downwelling and upwelling LW fluxes are used to re-calculate NLW. As ISCCP FD dataset albedo, AOD and incoming shortwave radiation did not show significant differences from MODIS or the surface measurements, the original incoming and outgoing SW fluxes from the ISCCP FD dataset are used to calculate NSW. Because of the small reduction in net LW (less negative value), the refined Rn are larger than in the original ISCCP FD values. For instance, in grid 1 at 09:00 UTC the mean yearly net LW value changed from  $-170.0 \text{ W/m}^2$  to  $-121.7 \text{ W/m}^2$  and, thus, the mean yearly Rn increased from  $364.7 \text{ W/m}^2$  to  $413.0 \text{ W/m}^2$  (Table 5 and 6). Grid 1 shows the largest differences and grid 5 shows the least differences. The mean difference of net LW varies from  $17.8$  to  $35 \text{ W/m}^2$  at different times of the day. The largest difference values occur at 9:00 and 12:00 and the smallest differences occur at 0:00 and 21:00 UTC (09:00 UTC is 12:30 local time). Summer and winter refined Rn (NLW) show larger values (less negative values) in all grids compared to the original ISCCP FD dataset. There are exceptions in grid 5 for both NLW and Rn during the summer, where Rn is smaller than the original ISCCP FD Rn for all 3-hour intervals except at 3:00 and 9:00 UTC. This is due to the large portion of the ISCCP FD grid area covered by ocean, the sub-grids on land show larger Rn compared to ISCCP FD like the other grids.

In the winter, the refined Rn values differ from the original ISCCP FD values by between  $4.64$ - $61.5 \text{ W/m}^2$  in all grids. This difference for summertime is about  $1.06$  to  $41.88 \text{ W/m}^2$  in grids 1 to 4 and about  $-10.2$  to  $2.47 \text{ W/m}^2$  in grid 5. Mean refined daily Rn difference from ISCCP FD ranges from  $31.8$  to  $246.1 \text{ W/m}^2$ , which is about  $11.1$  to  $39.2 \%$  relative to the original ISCCP FD values. The smallest difference occurs in grid 5 and the largest difference occurs in grid 1. Daily Rn differences are larger in winter than in summer. In Figure 6, the refined and original Rn at 9:00 UTC in 15<sup>th</sup> August is presented.

## **4. Conclusions**

Direct global estimates of surface net radiation that resolve regional and weather-scale variability with reasonable accuracy have become available based on satellite data sets within the past couple of decades. The main limitation is still the accuracy of the input data sets. Zhang et al. (Zhang et al., 2007, 2006, 2004, 1995) show that the leading uncertainties in the surface fluxes are now more associated with uncertainties in the near-surface atmospheric and the surface properties. Net fluxes with higher spatial resolution and more accuracy than a global dataset like ISCCP FD dataset is needed in agricultural meteorology to estimate ET. This motivated the current study to refine ISCCP FD radiation dataset to achieve higher spatial resolution while preserving its 3-hr time resolution.

Our comparison of the ISCCP FD and AIRS near-surface air ( $T_a$ ) and surface skin ( $T_s$ ) temperatures with surface measurements and supplemented by MODIS skin temperature data in the Fars Province of Iran showed that the AIRS  $T_a$  and  $T_s$  data had better accuracy than ISCCP FD dataset (less bias at higher values, more day-night consistency, better results when surface temperature inversions occur), when compared at the same spatial resolution (280 km), and better agreement with surface temperature measurements at its higher spatial resolution (45 km). Although the much higher spatial resolution (1 km) MODIS values of  $T_s$  did not agree better with surface measurements, the comparison did suggest that the 45 km AIRS results resolved much of the smaller spatial scale variations. A further reason to prefer the AIRS product is that it gives both physically consistent values of  $T_a$  and  $T_s$ .

However, the twice-daily sampling of AIRS product from the sun-synchronous Aqua orbit (reduced further by clouds) means that the diurnal variations of temperature, especially important in an arid environment like Iran, are not resolved, whereas the ISCCP FD data has 3-hr sampling under both cloudy and clear conditions. Since the temperature differences between ISCCP FD and AIRS were not too large, we developed a procedure using AIRS products to refine the ISCCP FD LW fluxes to achieve 45 km sampling while retaining the 3-hr sampling. The refined NLW has somewhat smaller negative value than the original ISCCP FD values: differences in all grids were between 17.8-35 W/m<sup>2</sup>. The differences are largest during daytime and least at night. The refinement also seems to be an improvement during wintertime when surface temperature inversion are common.

Although the ISCCP FD downwelling SW fluxes agreed well with surface measurements, we investigated possible improvements considering an alternate AOD dataset from MODIS. The differences of MODIS and ISCCP FD AOD showed no systematic relationship to the differences of ISCCP FD downwelling SW fluxes with surface measurement, so changing AOD inputs would not improve agreement. We also compared MODIS and ISCCP FD surface albedo values: the difference were between 0.02 to 0.07. Since the difference is mostly at longer wavelengths, it does not cause significant changes in upwelling SW (Zhang et al., 2007). Therefore, we retained the original ISCCP FD NSW estimates.

Refined Rn values at 45 km and 3-hr resolution were calculated, producing an overall increase compared with the original ISCCP FD values of 4.64-61.5 W/m<sup>2</sup> in summertime and 1.06-41.88 W/m<sup>2</sup> in wintertime.

In conclusion, the relatively low spatial resolution of global net radiation data products can be improved using other sources of data to replace the leading inputs and refine the flux estimates.

**Acknowledgments:** The corresponding author acknowledges Bu-Ali Sina University (Hamedan, Iran) and the NOAA-CREST at City University of New York support in this research. F.G. is supported by Bu-Ali Sina University and the CUNY-CREST Institute support. W.B.R. is supported by NASA Grant NNX13AI22A.

## References

- Arya, S.P., 2001. Introduction to Micrometeorology, second. ed, International Geophysics Series. Academic Press. doi:10.4043/13298-MS
- Boegh, E., Soegaard, H., Thomsen, A., 2002. Evaluating evapotranspiration rates and surface conditions using Landsat TM to estimate atmospheric resistance and surface resistance. Remote Sens. Environ. 79, 329–343. doi:10.1016/S0034-4257(01)00283-8
- Jimenez, C., Prigent, C., Catherinot, J., Rossow, W., Liang, P., Moncet, J.L., 2012. A comparison of ISCCP land surface temperature with other satellite and in situ observations. J. Geophys. Res. Atmos. 117, 1–8. doi:10.1029/2011JD017058



- Monteith, J., 1965. On the assessment of surface heat flux and evaporation using large-scale parameters. *Symp. Soc. Exp. Biol* 100, 81–92.
- Nishida, K., Nemani, R.R., Running, S.W., Glassy, J.M., 2003. An operational remote sensing algorithm of land surface evaporation. *J. Geophys. Res.* 108, 4270. doi:10.1029/2002JD002062
- Priestley, C., Taylor, R., 1972. On the assessment of surface heat flux and evaporation using large-scale parameters. *Mon. Weather Rev.* 100, 81–92. doi:10.1175/1520-0493(1972)100<0081:OTAOSH>2.3.CO;2
- Rossow, W.B., Garder, L.C., 1993. Validation of ISCCP cloud detections. *J. Clim.* 6, 2370–2393. doi:http://dx.doi.org/10.1175/1520-0442(1993)006<2370:VOICD>2.0.CO;2
- Rossow, W.B., Schiffer, R. a., 1991. ISCCP Cloud Data Products. *Bull. Am. Meteorol. Soc.* doi:10.1175/1520-0477(1991)072<0002:ICDP>2.0.CO;2
- Sayer, A.M., Hsu, N.C., Bettenhausen, C., Jeong, M.J., 2013. Validation and uncertainty estimates for MODIS Collection 6 “deep Blue” aerosol data. *J. Geophys. Res. Atmos.* 118, 7864–7872. doi:10.1002/jgrd.50600
- Shuttleworth, W.J., Wallace, J.S., 1985. Evaporation From Sparse Crops - An Energy Combination Theory. *Q. J. R. Meteorol. Soc.* 111, 839–855. doi:10.1002/qj.49711146910
- Su, Z., 2002. The Surface Energy Balance System ( SEBS ) for estimation of turbulent heat fluxes To cite this version : The Surface Energy Balance System ( SEBS ) for estimation of turbulent heat fluxes. *Hydrol. Earth Syst. Sci. Discuss. Eur. Geosci. Union* 6, 85–100. doi:hal-00304651
- Zhang, Y., Rossow, W.B., LACIS, A.A., 1995. Calculation of Surface and Top of Atmosphere Radiative Fluxes From Physical Quantities Based on Isccp Data Sets .1. Method and Sensitivity To Input Data Uncertainties. *J. Geophys. Res.* 100, 1149–1165. doi:10.1029/94JD02747
- Zhang, Y., Long, C.N., Rossow, W.B., Dutton, E.G., 2010. Exploiting diurnal variations to evaluate the ISCCP-FD flux calculations and radiative-flux-analysis-processed surface observations from BSRN, ARM, and SURFRAD. *J. Geophys. Res. Atmos.* 115, 1–21. doi:10.1029/2009JD012743
- Zhang, Y., Rossow, W.B., Lacis, A. a., Oinas, V., Mishchenko, M.I., 2004. Calculation of radiative fluxes from the surface to top of atmosphere based on ISCCP and other global data

sets: Refinements of the radiative transfer model and the input data. *J. Geophys. Res. D Atmos.* 109, 1–27. doi:10.1029/2003JD004457

Zhang, Y., Rossow, W.B., Stackhouse, P.W., 2007. Comparison of different global information sources used in surface radiative flux calculation: Radiative properties of the surface. *J. Geophys. Res. Atmos.* 112, D01102. doi:10.1029/2005JD007008

Zhang, Y., Rossow, W.B., Stackhouse, P.W., 2006. Comparison of different global information sources used in surface radiative flux calculation: Radiative properties of the surface. *J. Geophys. Res. Atmos.* 112, D01102. doi:10.1029/2005JD007008

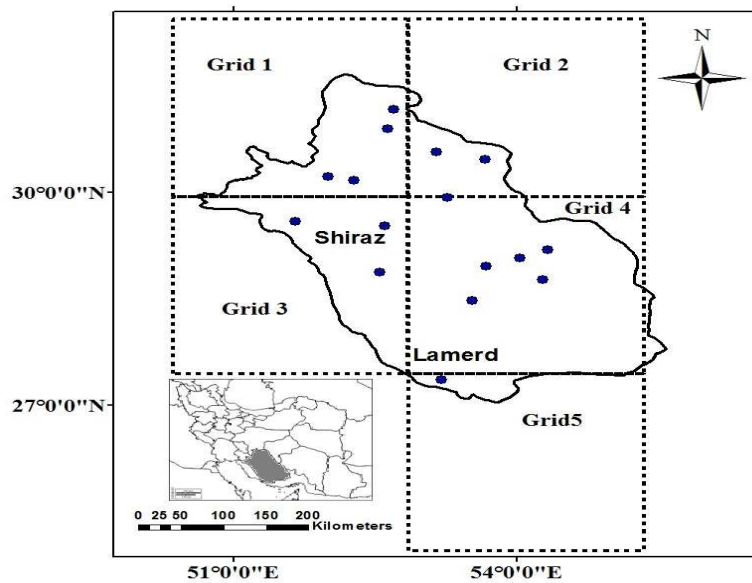


Figure 1. Geographical distribution of the automated weather stations and the ISCCP FD grids in the Fars Province, Iran

Table 1. Average of difference (RMS of difference) values in AIRS and ISCCP FD dataset  $T_a$  comparison with measured  $T_a$  (K)

Source of Data		Day Average (RMS) of difference	Night Average (RMS) of difference
ISCCP FD dataset	AIRS	-3.1 (5.3)	-2.4 (4.6)
	Grid 1	3.9(7.4)	3.1 (7.0)
	Grid 2	4.4 (5.4)	5.5 (6.5)
	Grid 3	3.5 (6.8)	5.1 (5.8)
	Grid 4	4.4 (5.7)	3.3 (4.9)

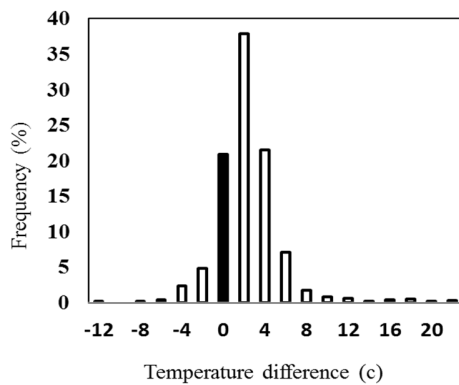
Grid 5

-2.0 (6.2)

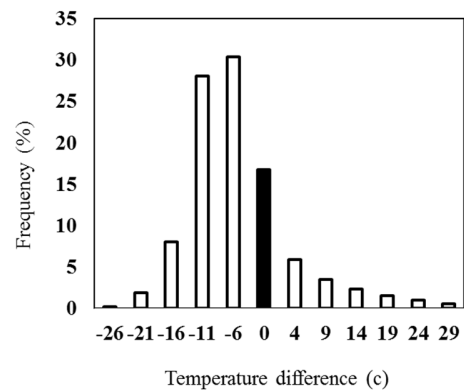
3.0 (5.0)

Table 2. Average of difference (RMS of Difference) values in satellite and ISCCP FD dataset  $T_s$  comparison with measured soil temperature (K)

Source of data	Day Average (RMS) of difference	Night Average (RMS) of difference
Terra	12.6 (12.9)	-10.8 (11.9)
Aqua	11.5 (5.4)	-11.1 (10.8)
AIRS	10.0 (9.1)	-1.9 (4.3)
ISCCP FD dataset	Grid 1	12.3 (11.2)
	Grid 2	14.0 (10.6)
	Grid 3	13.6 (8.9)
	Grid 4	11.0 (9.5)
	Grid 5	1.0 (6.4)



(a)



(b)

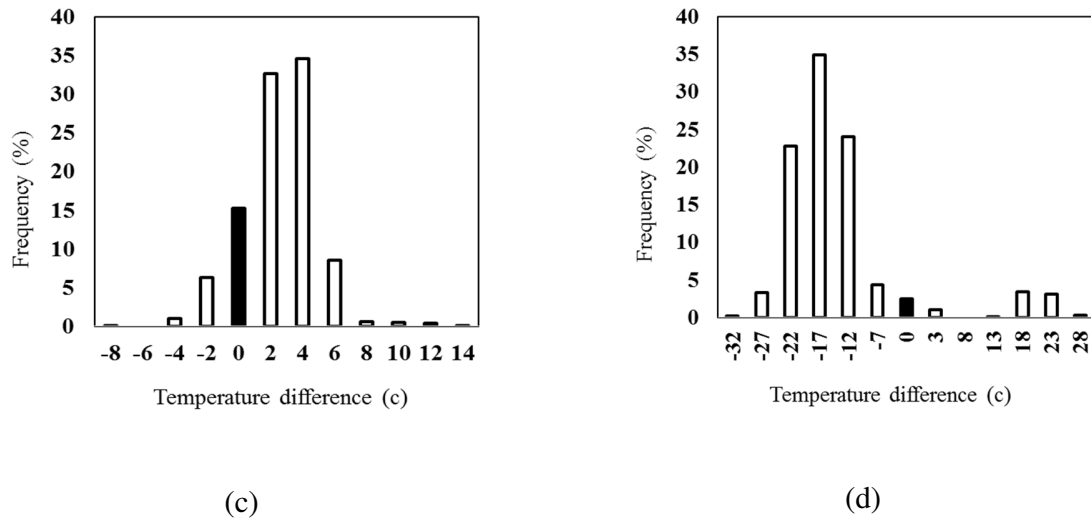


Figure 2. AIRS histograms of  $\Delta T$  in winter daytime (a) and nighttime (b) and summer daytime (c) and nighttime (d)

Table 3. ISCCP FD dataset, observed incoming shortwave radiation and the difference of two datasets ( $\Delta SW$ ) in the studied area ( $W/m^2$ )

	<b>Time</b>	<b>ISCCP FD Dataset</b>	<b>Observed Data</b>	<b><math>\Delta SW</math></b>	<b>% of difference</b>
Grid 1	3:00	94.2	102.4	8.2	8.0
	6:00	604.8	590.8	-14.0	-2.4
	9:00	771.0	753.0	-17.9	-2.4
	12:00	402.4	420.6	18.2	4.3
Grid 5	3:00	81.2	97.3	16.1	16.5
	6:00	606.4	524.8	-81.7	-15.6
	9:00	812.3	730.0	-82.3	-11.3
	12:00	436.5	398.5	-38.0	-9.5

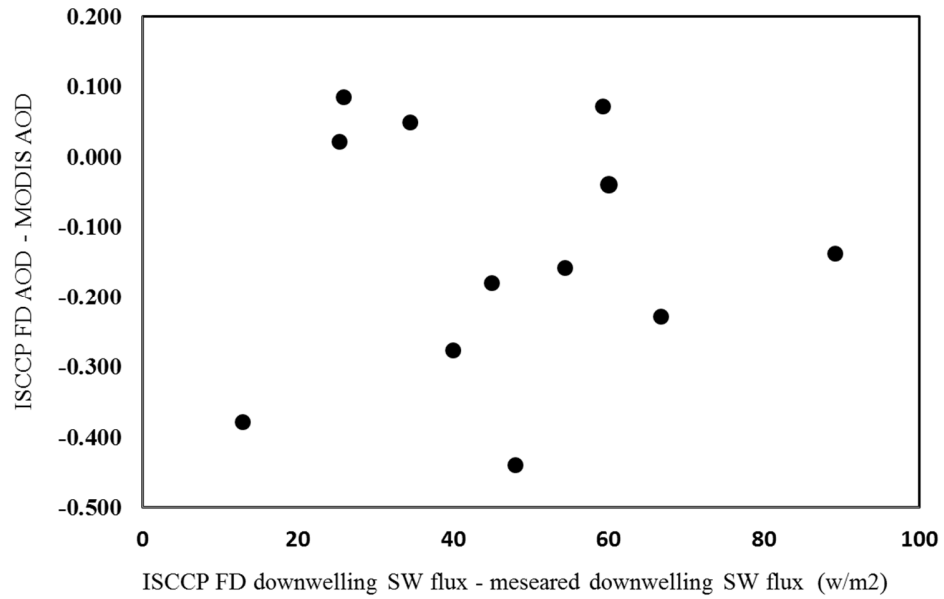


Figure 3. The correlation of AOD difference of the two datasets with the difference of the ISCCP FD and the surface-measured downwelling SW fluxes

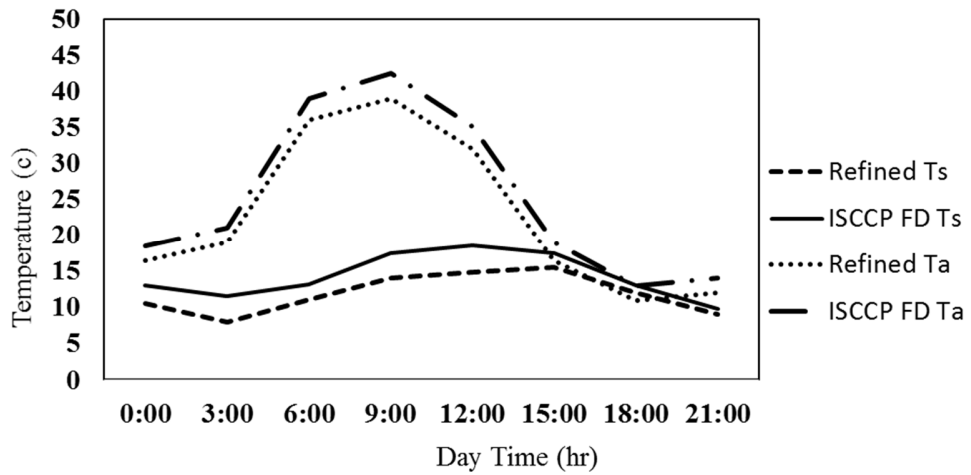
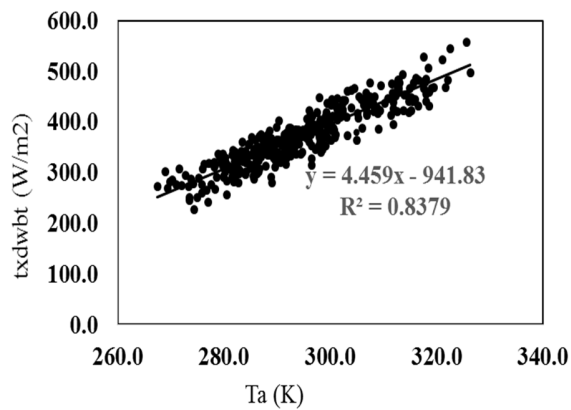


Figure 4. ISCCP FD temperatures and refined  $T_a$  and  $T_s$  data using AIRS' sensor for

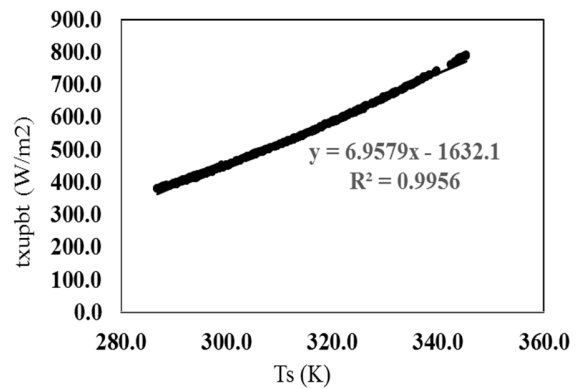
July 13, 2009

Table 4. ISCCP FD and refined ISCCP FD  $T_a$  and  $T_s$  dataset with the corresponding differences ( $\Delta T$ )

Grid	time	$T_a$ ( $^{\circ}\text{C}$ )			$T_s$ ( $^{\circ}\text{C}$ )		
		original data	refined data	$\Delta T$	original data	refined data	$\Delta T$
G1	0:00	12.8	8.7	-4.1	14.2	8.8	-5.4
	3:00	11.0	6.5	-4.4	15.2	9.7	-5.5
	6:00	15.0	11.3	-3.7	30.1	21.3	-8.8
	9:00	22.0	19.2	-2.9	39.5	30.1	-9.5
	12:00	22.4	20.6	-1.9	31.7	24.6	-7.0
	15:00	20.7	18.7	-1.9	17.8	12.0	-5.8
	18:00	17.5	14.6	-2.9	14.8	9.1	-5.8
	21:00	14.5	11.0	-3.4	14.3	8.8	-5.5
G5	0:00	23.8	24.6	0.9	27.4	23.3	-4.1
	3:00	23.9	24.6	0.7	27.4	26.0	-1.4
	6:00	28.1	26.2	-1.9	30.2	26.5	-3.7
	9:00	29.2	26.8	-2.3	34.2	30.2	-4.0
	12:00	28.9	26.8	-2.1	31.8	25.7	-6.1
	15:00	27.1	25.9	-1.2	27.5	22.3	-5.2
	18:00	25.9	25.3	-0.5	27.2	23.3	-3.9
	21:00	24.7	25.1	0.3	27.4	24.9	-2.5



a



b

Figure 5.  $T_a$  correlation with downwelling longwave radiation (a) and  $T_s$  correlation with upwelling longwave radiation (b)

Table 5. Annual average of original and refined ISCCP FD net LW in studied grids (W/m<sup>2</sup>)

Time	G1		G2		G3		G4		G5	
	Original NLW	Refined NLW	Original NLW	Refined NLW	Original NLW	Refined NLW	Original NLW	Refined NLW	Original NLW	Refined NLW
0:00	-63.7	-43.4	-59.6	-45.0	-84.5	-57.1	-77.3	-58.3	-94.6	-79.1
3:00	-74.5	-57.8	-79.1	-60.9	-81.9	-54.0	-81.6	-61.4	-94.1	-76.4
6:00	-145.9	-111.7	-165.8	-150.4	-92.7	-71.4	-136.2	-103.5	-93.6	-81.2
9:00	-170.0	-121.7	-201.4	-160.6	-114.1	-89.0	-172.1	-129.5	-102.5	-83.4
12:00	-121.4	-78.2	-135.4	-107.4	-99.3	-76.2	-129.9	-87.6	-94.9	-76.8
15:00	-52.8	-25.0	-35.9	-33.7	-95.0	-75.4	-72.8	-40.8	-88.1	-75.0
18:00	-48.3	-27.1	-45.9	-33.2	-88.7	-66.3	-72.9	-46.1	-88.9	-72.6
21:00	-57.3	-38.7	-44.8	-37.2	-86.5	-65.3	-71.9	-48.1	-91.4	-73.2
Max	-48.3	-25.0	-35.9	-33.2	-81.9	-54.0	-71.9	-40.8	-88.1	-72.6
Min	-170.0	-121.7	-201.4	-160.6	-114.1	-89.0	-172.1	-129.5	-102.5	-83.4
Average	-91.7	-63.0	-89.1	-85.5	-92.8	-69.3	-101.8	-71.9	-93.5	-77.2

Table 6. Annual average of refined and ISCCP FD net radiation in studied grids (W/m<sup>2</sup>)

Time	G1		G2		G3		G4		G5	
	Original Rn	Refined Rn	Original Rn	Refined Rn	Original Rn	Refined Rn	Original Rn	Refined Rn	Original Rn	Refined Rn
0:00	-63.7	-43.4	-59.6	-45.0	-84.5	-57.1	-77.3	-58.3	-94.6	-79.1
3:00	-2.3	14.4	18.0	35.5	-22.8	5.1	4.5	24.7	-3.9	13.8
6:00	290.9	325.0	320.1	335.0	403.7	425.0	338.1	370.8	495.6	507.9
9:00	364.7	413.0	356.1	395.8	574.3	599.4	375.1	417.7	600.4	619.5
12:00	194.3	237.5	172.8	199.8	272.5	295.6	202.0	244.2	275.1	293.2
15:00	-31.5	-3.7	-19.9	-17.7	-73.2	-53.5	-54.2	-22.3	-73.7	-60.7
18:00	-48.3	-27.1	-44.7	-32.3	-88.7	-66.2	-72.9	-46.1	-88.9	-72.7
21:00	-57.3	-38.7	-43.4	-36.0	-86.5	-65.3	-71.9	-48.1	-91.4	-73.2

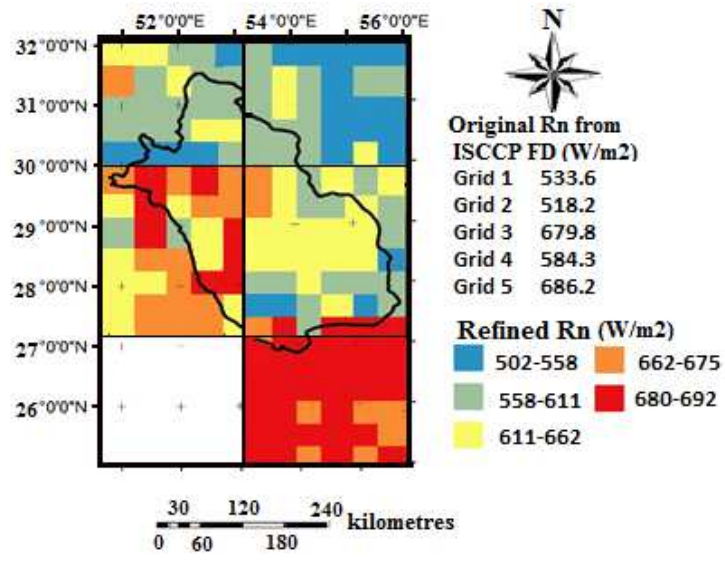


Figure 6. The refined and original Rn in studied area in 15<sup>th</sup> August at 9:00 UTC